JACS
JOURNAL OF THE AMERICAN CHEMICAL SOCIETY

Article

pubs.acs.org/JACS

Syntheses and Structural Characterizations of Inorganic *ansa*-Metallocene Analogues: *ansa*-Ferratricarbadecaboranes

Brendan Gleeson, Patrick J. Carroll, and Larry G. Sneddon*

Department of Chemistry, University of Pennsylvania, Philadelphia, Pennsylvania 19104-6323, United States

Supporting Information

ABSTRACT: New linked cyclopentadienyl-tricarbadecaboranyl and bis-tricarbadecaboranyl dianions have been used to form the first examples of *ansa*-metallatricarbadecaboranyl complexes. The hybrid cyclopentadienyl-tricarbadecaboranyl dianion, $Li_2^+[6\text{-}C_5H_4\text{-}(CH_2)_2\text{-}nido\text{-}5,6,9\text{-}C_3B_7H_9]^{2-}$ (**1**), was produced by an initial carbon-insertion reaction of a nitrile-substituted cyclopentadiene with the *arachno*-4,6-$C_2B_7H_{12}^-$ anion, followed by deprotonation to the dianion with LiH. The linked-cage bis-tricarbadecaboranyl dianion, $Li_2^+[6,6'\text{-}(CH_2)_2\text{-}nido\text{-}(5,6,9\text{-}C_3B_7H_9)_2]^{2-}$ (**2**), was produced by a similar carbon-insertion route involving the reaction of two equivalents of *arachno*-4,6-$C_2B_7H_{12}^-$ with succinonitrile. The reaction of **1** with an equivalent of $FeCl_2$ produced the hybrid complex, *ansa*-(2-$(CH_2)_2$)-(1-η^5-C_5H_4-*closo*-1,2,3,4-$C_3B_7H_9$)Fe (**3**), with a crystallographic determination confirming the formation of a sandwich structure where the ring and cage are linked by the *ansa* $-CH_2CH_2-$ group with attachment to the cage at the C2 carbon. The reaction of **2** with $FeCl_2$ produced three isomeric *ansa*-$(CH_2)_2$-ferrabistricarbadecaboranyl sandwich complexes, *ansa*-$(CH_2)_2$-(*closo*-$C_3B_7H_9)_2$Fe (**4**, **5** and **6**). Crystallographic determinations showed that in **4**, the two tricarbadecaboranyl ligands are linked by the *ansa*-CH_2CH_2- group at the C2 and C2′ cage carbons, whereas in **5** and **6** they are linked at their C2 and C4′ carbons, with the structures of **5** and **6** differing in the relative positions of the C4′ carbons in the two cages of each complex. The structural determinations also showed that, depending upon the linking position of the *ansa*-tether, constraints in cage-orientation, such as observed in **4**, produce unfavorable intercage steric interactions. However, the cage fragments in these complexes can readily undergo a cage-carbon migration that moves one -carbon and its tether linkage to the more favorable 4-position. This isomerization reduces the cage steric interactions and produces configurations, such as those found for **5** and **6**, where the iron cage bonding is enhanced as a result of the binding effect of the tether.

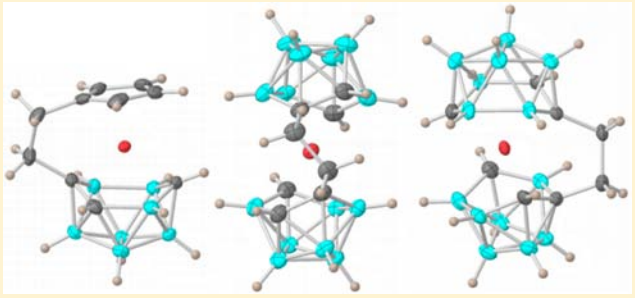

INTRODUCTION

With the same −1 charge and a similar coordination ability as that of the cyclopentadienide $C_5H_5^-$ anion, the tricarbadecaboranide anions, 6-R-5,6,9-*nido*-$C_3B_7H_9^-$ (R = Me or Ph) have been used to generate a wide range of sandwich complexes, with these complexes exhibiting both enhanced oxidative and hydrolytic stabilities and substantially different electrochemical and chemical activities compared to their metallocene analogues.[1] Owing to their increased stabilities and constrained geometries, *ansa*-ligated metallocenes,[2] where the two cyclopentadienyl rings are linked by either single or multiatom tethers as well as *ansa*-ligated metalladicarbaboranyl complexes,[3] have received recent intense research activity, with their unique properties giving rise to applications as diverse as new stereoselective catalysts, chelating agents for metal separations, and biomedical reagents. The previously unknown *ansa*-metallatricarbadecaboranes should likewise have similar potential applications with properties that could again complement those of traditional cyclopentadienyl-based *ansa*-complexes. In this paper, we report the synthesis of both new linked cyclopentadienyl-tricarbadecaboranyl and bis-tricarbadecaboranyl dianions, along with their use to form the first examples of such *ansa*-metallatricarbadecaboranyl complexes.

EXPERIMENTAL SECTION

Unless otherwise noted, all reactions and manipulations were performed in dry glassware under nitrogen or argon atmospheres using the high-vacuum or inert-atmosphere techniques described by Shriver and Drezdzon.[4]

Materials. The 1,3-cyclopentadiene-1-propanenitrile was prepared by a previously reported method.[5] Iron(II) chloride, lithium hydride, sodium cyclopentadienide (2.0 M solution in THF), succinonitrile, spectrochemical grade dichloromethane, and hexanes (Fisher) were used as received. The *arachno*-4,6-$C_2B_7H_{13}$ was prepared as described previously.[6] THF was freshly distilled from sodium-benzophenone ketyl. All other solvents were used as received unless noted otherwise.

Physical Measurements. The ^{11}B NMR spectra at 128.4 MHz and ^1H NMR spectra at 400.1 MHz were obtained on a Bruker DMX-400 spectrometer equipped with appropriate decoupling accessories. All ^{11}B chemical shifts are referenced to external $BF_3{\cdot}O(C_2H_5)_2$ (0.0 ppm) with a negative sign indicating an upfield shift. All ^1H chemical shifts were measured relative to internal residual protons in the lock

Received: June 14, 2013
Published: August 9, 2013

dx.doi.org/10.1021/ja405977q | J. Am. Chem. Soc. 2013, 135, 12407−12413

solvents and are referenced to Me_4Si (0.0 ppm). High- and low-resolution mass spectra employing chemical ionization with negative ion detection were obtained on a Micromass AutoSpec high-resolution mass spectrometer. IR spectra were obtained on a Perkin-Elmer Spectrum 100 FT-IR spectrometer. Elemental analyses were carried out at the MicroAnalytical Facility at UC Berkeley, CA. Melting points were determined using a standard melting point apparatus and are uncorrected.

Ligand Syntheses. *$Li_2^+[6\text{-}C_5H_4\text{-}(CH_2)_2\text{-}nido\text{-}5,6,9\text{-}C_3B_7H_9]^{2-}$ (1).* LiH (35 mg, 4.44 mmol) was added to a stirring THF (20 mL) solution of *arachno*-4,6-$C_2B_7H_{13}$ (500 mg, 4.44 mmol) under N_2 at room temperature. The solution was monitored by NMR until ∼95% complete. The solution was then filtered through a frit under N_2 to remove excess LiH. A THF solution of 1,3-cyclopentadiene-1-propanenitrile (2.41 g, 20.4 mmol in 20 mL THF) was added via syringe. The reaction mixture was stirred at reflux for 36 h, then cooled, and filtered through a frit under N_2. The resulting $Li^+[6\text{-}C_5H_5\text{-}(CH_2)_2\text{-}nido\text{-}5,6,9\text{-}C_3B_7H_9]^-$ anion was not isolated but immediately reacted with an excess of LiH and stirred at room temperature for 24 h under N_2. The solution was again filtered through a frit under N_2 to remove excess LiH. The resulting $Li_2^+[6\text{-}C_5H_4\text{-}(CH_2)_2\text{-}nido\text{-}5,6,9\text{-}C_3B_7H_9]^{2-}$ (**1**) was not isolated but instead stored as a stock solution until use. The concentration of the solution and the yield (72%, 0.08 M) was determined by integrating the resonances in the ^{11}B NMR spectrum of a $B_{10}H_{14}$ sample of known concentration and comparing that value with the integrated value of the resonances of the stock solution. $^{11}B\{^1H\}$ NMR for **1**: 6.8 (1B), 3.7 (1B), −5.4 (1B), −10.7 (1B), −13.0 (1B), −24.7 (1B), −31.7 (1B) ppm.

$Li_2^+[6,6'\text{-}(CH_2)_2\text{-}nido\text{-}(5,6,9\text{-}C_3B_7H_9)_2]^{2-}$ (2). LiH (35 mg, 4.44 mmol) was added to a stirring THF (20 mL) solution of *arachno*-4,6-$C_2B_7H_{13}$ (500 mg, 4.44 mmol) under N_2 at room temperature. The solution was monitored by NMR until ∼95% complete. The solution was then filtered through a frit under N_2 to remove excess LiH. A THF solution of succinonitrile (176 mg, 2.22 mmol in 10 mL THF) was added via syringe. The reaction mixture was stirred at reflux for 24 h, then cooled, and filtered through a frit under N_2. The resulting Li_2^+ $[6\text{-}(CH_2)_2\text{-}nido\text{-}(5,6,9\text{-}C_3B_7H_9)_2]^{2-}$ was not isolated but instead stored as a stock solution until use. The concentration of the solution and the yield (81%, 0.09 M) was determined by integrating the resonances in the ^{11}B NMR spectrum of a $B_{10}H_{14}$ sample of known concentration and comparing that value with the integrated value of the resonances of the stock solution. $^{11}B\{^1H\}$ NMR for **2**: 7.3 (1B), 3.2 (1B), −4.9 (1B), −10.5 (1B), −13.1 (1B), −25.2 (1B), −32.0 (1B) ppm.

***ansa*-Ferratricarbadecaborane Syntheses.** *ansa-(2-$(CH_2)_2$)-(1-η^5-C_5H_4)-closo-1,2,3,4-$C_3B_7H_9Fe$ (3).* A THF solution of **1** (30 mL of a 0.08 M solution, 2.40 mmol) was added dropwise to a stirring THF (20 mL) solution of $FeCl_2$ (304 mg, 2.40 mmol) under N_2. After stirring for 24 h at reflux, ^{11}B NMR analysis showed that the reaction solution contained unreacted **1**, some cage degradation products (primarily *arachno*-4,6-$C_2B_7H_{13}$) and a single ferratricarbadecaboranyl product. The reaction mixture was then exposed to air and filtered through a short silica gel plug using CH_2Cl_2 as an eluent. The solvent was vacuum evaporated and the oily brown residue was redissolved in 5 mL of CH_2Cl_2 and eluted through a silica gel column using 1:1 hexanes/CH_2Cl_2 as the eluent to give **3** in 26% yield (167 mg, 0.62 mmol); blue; R_f 0.76; mp 201°C. Anal. calcd: C, 44.69; H, 6.37; found: C, 44.64; H, 6.50. NCI HRMS m/z for $C_{10}H_{17}B_7Fe^-$: calcd 270.1331, found 270.1336. ^{11}B NMR ($CDCl_3$, ppm, J = Hz) −1.2 (1, d, 157), −3.1 (1, d, 166), −8.7 (1, d, 149), −13.9 (1, d, 149), −26.4 (1, d, 141), −29.5 (1, d, 157), −33.1 (1, d, 157). ^1H NMR ($CDCl_3$, ppm) 6.63 (1, s, C3*H*), 5.11 (1, m, C_5H_4), 4.76 (1, m, C_5H_4), 4.58 (2, m, C_5H_4, CH_2), 4.18 (1, m, C_5H_4), 3.75 (1, m, CH_2), 3.07 (1, m, CH_2), 2.73 (1, m, CH_2), 1.59 (1, s, C4*H*). IR (KBr, cm^{-1}): 3098 (w), 3083 (w), 2924 (w), 2859 (w), 2572 (w), 2540 (s), 1467 (w), 1437 (w), 1322 (w), 1105 (w), 1029 (mw), 941 (w), 855 (w), 726 (w), 653 (w).

ansa-$(CH_2)_2$-(closo-$C_3B_7H_9)_2Fe$ Complexes (4–6). A THF solution of **2** (30 mL of a 0.09 M solution, 2.70 mmol) was added dropwise to a stirring THF (20 mL) solution of $FeCl_2$ (342 mg, 2.70 mmol) under N_2. After stirring for 24 h at reflux, ^{11}B NMR analysis showed that the reaction solution contained a mixture of ferratricarbaboranyl complexes, along with unreacted **2** and some cage-degradation products (primarily *arachno*-4,6-$C_2B_7H_{13}$). TLC analysis of the reaction solution at this point confirmed the formation of three ferratricarbadecaboranyl complexes. The reaction mixture was exposed to air and then filtered through a short silica gel plug using CH_2Cl_2 as an eluent. The solvent was vacuum evaporated, and the oily brown residue was redissolved in 5 mL of CH_2Cl_2 and eluted through a silica gel column using 1:1 hexanes/CH_2Cl_2 as the eluent to give the three isomeric products **4**–**6**.

4: 13% yield (118 mg, 0.36 mmol); brown; R_f 0.78; mp 174–176 °C, Anal. calcd: C, 29.49; H, 6.80; found: C, 29.66; H, 6.84. NCI HRMS m/z for $C_8H_{22}B_{14}Fe^-$: calcd: 328.2374; found: 328.2376. ^{11}B NMR ($CDCl_3$, ppm, J = Hz) 11.0 (1, d, 168), 0.5 (1, d, 168), −1.0 (1, d, 168), −2.6 (1, d, 168), −18.1 (1, d, 136), −18.4 (1, d, 186), −32.8 (1, d, 168). ^1H NMR ($CDCl_3$, ppm,) 9.82 (1, s, C3*H*), 4.27 (2, m, CH_2), 3.43 (2, m, CH_2), 2.70 (s, 2, C4*H*). IR (KBr, cm^{-1}): 3058 (w), 3032 (w), 2968 (w), 2942 (w), 2870 (w), 2635 (w), 2603 (s), 2565 (s), 1448 (m), 1322 (w), 1276 (w), 1142 (m), 1096 (w), 957 (m), 941 (w), 915 (w), 897 (w), 860 (m), 765 (w), 728 (m), 682 (w), 650 (w).

5: 9% yield (75 mg, 0.23 mmol); red; R_f 0.74; mp 164 °C, Anal. calcd: C, 29.49; H, 6.80; found: C, 30.08; H, 6.78. NCI HRMS m/z for $C_8H_{22}B_{14}Fe^-$: calcd: 328.2374; found: 328.2373. ^{11}B NMR ($CDCl_3$, ppm, J = Hz) 8.1 (1, d, 155), 5.4 (1, d, 155), 2.2 (1, d, 207), 0.5 (1, d, 155), −0.4 (1, d, 135), −1.5 (1, d, 145), −9.6 (1, d, 145), −10.6 (1, d, 145), −21.5 (1, d, 135), −22.3 (1, d, 155), −23.8 (2, d, 175), −25.4 (2, d, 185). ^1H NMR ($CDCl_3$, ppm,) 7.88 (1, s, C3*H* or C2*H*), 7.33 (1, s, C3*H* or C2*H*), 6.84 (1, s, C3*H* or C2*H*), 4.08 (1, m, CH_2), 3.12 (2, m, CH_2), 2.06 (1, m, CH_2), 1.83 (1, s, C4*H*). IR (KBr, cm^{-1}): 3073 (w), 3031 (w), 2961 (w), 2935 (w), 2871 (w), 2856 (w), 2582 (s), 2541 (w), 1455 (w), 1437 (w), 1262 (w), 1139 (w), 1123 (w), 1097 (m), 1053 (m), 1034 (m), 952 (m), 934 (m), 858 (m), 822 (w), 718 (m), 694 (w).

6: 11% yield (93 mg, 0.29 mmol); red; R_f 0.82; mp 119 °C, Anal. calcd: C, 29.49; H, 6.80; found: C, 30.11; H, 6.83. NCI HRMS m/z for $C_8H_{22}B_{14}Fe^-$: calcd: 328.2374; found: 328.2379. ^{11}B NMR ($CDCl_3$, ppm, J = Hz) 9.1 (1, d, 162), 6.7 (1, d, 162), −0.4 (2, d, 170), −2.3 (1, d, 178), −4.3 (1, d, 153), −7.0 (1, d, 162), −9.9 (1, d, 153), −20.2 (1, d, 121), −21.2 (2, d, 153), −23.4 (1, d, 186), −25.0 (1, d, 186), −31.7 (1, d, 162). ^1H NMR ($CDCl_3$, ppm,) 7.60 (1, s, C3*H* or C2*H*), 6.94 (1, s, C3*H* or C2*H*), 6.44 (1, s, C3*H* or C2*H*), 3.78 (1, m, CH_2), 3.63 (1, m, CH_2), 3.04 (1, s, C4*H*), 2.96 (1, m, CH_2), 2.59 (1, m, CH_2). IR (KBr, cm^{-1}): 3060 (w), 3036 (w), 2932 (w), 2593 (s), 2565 (s), 1440 (w), 1276 (w), 1143 (w), 1099 (w), 1042 (w), 943 (m), 905 (w), 864 (w), 825 (m), 798 (w), 758 (w), 720 (m), 694 (w), 646 (w).

Thermal Conversion of 4 to 5. A 10 mg sample of **4** was sealed under vacuum in a glass tube. After the tube was submersed in an oil bath at 200 °C for 8 h, it was opened, and the contents completely dissolved in 2 mL of CH_2Cl_2. Analysis by ^{11}B NMR and TLC showed complete conversion to **5**.

Crystallographic Procedures. Single crystals were grown through slow solvent evaporation from dichloromethane solutions in air or through vapor–liquid diffusion of pentane into dichloromethane or trichloromethane solutions.

X-ray intensity data for **3** (Penn3410), **4** (Penn3414), **5** (Penn3419), and **6** (Penn3415) were collected on a Bruker APEXII CCD diffractometer employing graphite monochromated Mo–K_α radiation (λ = 0.71073 Å). Rotation frames were integrated using SAINT,[7] producing a list of unaveraged F^2 and $\sigma(F^2)$ values that were then passed to the SHELXTL[8] program package for further processing and structure solution on a Dell Pentium 4 computer. The intensity data were corrected for Lorentz and polarization effects and for absorption.

The structures were solved by direct methods (SIR97).[9] Refinement was by full-matrix least-squares based on F^2 using SHELXL-97.[10] All reflections were used during refinement (values of F^2 that were experimentally negative were replaced with F^2 = 0). All nonhydrogen atoms were refined anisotropically, and hydrogen atoms were refined isotropically. The identities of boron versus carbon cage atoms were

Table 1. Crystallographic Data Collection and Structure Refinement Information

	3	4	5	6
empirical formula	$C_{10}B_7H_{17}Fe$	$C_8B_{14}H_{22}Fe$	$C_8B_{14}H_{22}Fe$	$C_8B_{14}H_{22}Fe$
formula weight	268.76	325.45	325.45	325.45
crystal class	triclinic	monoclinic	triclinic	monoclinic
space group	$P\bar{1}$ (#2)	$P2_1/n$ (#14)	$P\bar{1}$ (#2)	$P2_1/c$ (#14)
Z	2	4	2	4
a, Å	6.5321(3)	7.8737(4)	8.0019(6)	8.8907(8)
b, Å	8.0627(3)	16.7333(10)	8.8512(7)	21.898(2)
c, Å	12.6859(5)	12.7705(6)	12.1961(10)	8.6690(8)
α, °	73.519(2)		99.761(3)	
β, °	84.233(2)	102.676(2)	96.347(4)	108.393(4)
γ, °	77.446(2)		105.058(3)	
V, Å^3	624.81(4)	1641.54(15)	811.15(11)	1601.5(3)
D_{calc}, g/cm^3	1.429	1.317	1.332	1.350
μ, mm^{-1}	1.172	0.899	0.909	0.921
λ, Å (Mo−K$_\alpha$)	0.71073	0.71073	0.71073	0.71073
crystal size, mm	0.25 × 0.20 × 0.08	0.38 × 0.30 × 0.08	0.48 × 0.38 × 0.32	0.28 × 0.22 × 0.12
F(000)	276	664	332	664
2θ angle, °	5.38−55.04	4.08−55.32	4.88−55.06	3.72−55.26
temperature, K	143(1)	143(1)	143(1)	143(1)
hkl collected	$-8 \le h \le 8$	$-10 \le h \le 10$	$-10 \le h \le 9$	$-11 \le h \le 11$
	$-10 \le k \le 10$	$-21 \le k \le 21$	$-11 \le k \le 11$	$-28 \le k \le 28$
	$-16 \le l \le 16$	$-16 \le l \le 16$	$-15 \le l \le 15$	$-11 \le l \le 11$
no. meas reflns	20 766	34 842	15 453	42 012
no. unique reflns	2852 (R_{int} = 0.0148)	3802 (R_{int} = 0.0205)	3640 (R_{int} = 0.0210)	3718 (R_{int} = 0.0203)
no. parameters	236	297	297	297
R^a indices	R_1 = 0.0283	R_1 = 0.0284	R_1 = 0.0328	R_1 = 0.0280
(all data)	wR_2 = 0.0827	wR_2 = 0.0680	wR_2 = 0.0854	wR_2 = 0.0728
R^a indices	R_1 = 0.0236	R_1 = 0.0255	R_1 = 0.0301	R_1 = 0.0270
($F > 2\sigma$)	wR_2 = 0.0707	wR_2 = 0.0658	wR_2 = 0.0829	wR_2 = 0.0720
GOF^b	1.231	1.067	1.228	1.102
final difference peaks, e/ Å^3	0.594, −0.732	0.456, −0.237	0.552, −0.372	0.604, −0.237

$^aR_1 = \sum||F_o| - |F_c||/\sum|F_o|$; $wR_2 = \{\sum w(F_o^2 - F_c^2)^2/\sum w(F_o^2)^2\}^{1/2}$. ^{b}GOF = $\{\sum w(F_o^2 - F_c^2)^2/(n-p)\}^{1/2}$.

straightforwardly assigned based on their characteristic thermal parameters and bond distances.

Crystal and refinement data are given in Table 1. Selected bond distances and angles are given in the figure captions.

RESULTS AND DISCUSSION

By employing the carbon-insertion method originally developed by Kang,[11,1a] the hybrid cyclopentadienyl-tricarbadecaboranyl dianion, $Li_2^+[6\text{-}C_5H_4\text{-}(CH_2)_2\text{-}nido\text{-}5,6,9\text{-}C_3B_7H_9]^{2-}$ (**1**), was produced by the sequence shown in Scheme 1. The initial formation of the linked $Li^+[6\text{-}C_5H_5\text{-}(CH_2)_2\text{-}nido\text{-}5,6,9\text{-}C_3B_7H_9]^-$ monoanion was achieved by the reaction of the nitrile-substituted cyclopentadiene with the *arachno*-4,6-$C_2B_7H_{12}^-$ anion. The reaction was monitored by ^{11}B NMR until the growth of the seven-line spectral pattern of the 6-R-*nido*-5,6,9-$C_3B_7H_9^-$ anion indicated the reaction was complete.[11] The addition of excess LiH to the monoanion solution then resulted in additional hydrogen evolution and the formation of the **1** dianion.

As shown in Scheme 2, the linked-cage bis-tricarbadecaboranyl dianion, $Li_2^+[6,6'\text{-}(CH_2)_2\text{-}nido\text{-}(5,6,9\text{-}C_3B_7H_9)_2]^{2-}$ (**2**),

Scheme 1. Synthesis of $Li_2^+[6\text{-}C_5H_4\text{-}(CH_2)_2\text{-}nido\text{-}5,6,9\text{-}C_3B_7H_9]^{2-}$ (1)

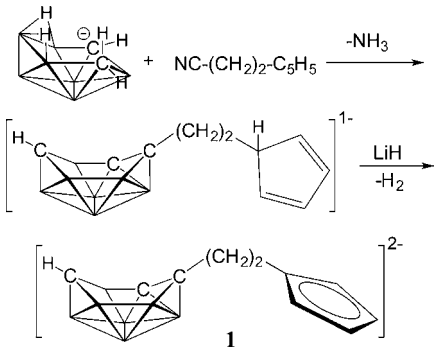

Scheme 2. Synthesis of $Li_2^+[6,6'\text{-}(CH_2)_2\text{-}nido\text{-}(5,6,9\text{-}C_3B_7H_9)_2]^{2-}$ (2)

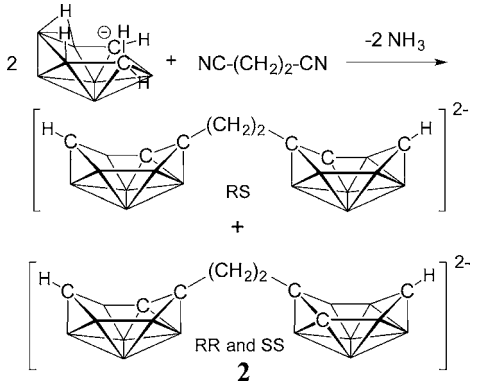

dx.doi.org/10.1021/ja405977q | J. Am. Chem. Soc. 2013, 135, 12407−12413

was produced by a similar carbon-insertion route involving the reaction of 2 equiv of *arachno*-4,6-$C_2B_7H_{12}^-$ with succinonitrile, with the final product again exhibiting a ^{11}B NMR spectrum characteristic of the 6-R-*nido*-5,6,9-$C_3B_7H_9^-$ anion.[11] Because the tricarbadecaborane cage is enantiomeric, the linked bis-cage product **2** is produced in the two forms shown in the Scheme 2 resulting from the RS, RR, and SS combinations of 6-R-*nido*-5,6,9-$C_3B_7H_9^-$ enantiomers. The **1** and **2** dianions were not isolated but were instead stored as stock solutions until use.

As shown in Scheme 3 (top), the hybrid *ansa*-cyclopentadienyl-ferratricarbadecaboranyl complex, *ansa*-(2-

Scheme 3. Syntheses of *ansa*-Complexes 3−6

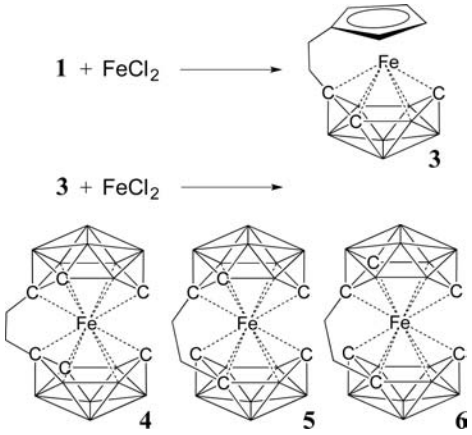

$(CH_2)_2$)-(1-η^5-C_5H_4-*closo*-1,2,3,4-$C_3B_7H_9$)Fe (**3**), was produced by the reaction of equivalent amounts of **1** and $FeCl_2$. Following purification by column chromatography, **3** was isolated as a crystalline blue solid.

The chemical shifts and seven doublet pattern exhibited in the ^{11}B NMR spectrum of **3** are quite similar to those of (1-η^5-C_5H_5)-*closo*-2-CH_3-1,2,3,4-$C_3B_7H_9$)Fe.[1a] Likewise, its ^{1}H NMR spectrum showed, in addition to the expected multiplet resonances of the η^5-C_5H_4 and the *ansa*-CH_2CH_2- linking group, two cage CH resonances, with the higher-field (1.59 ppm) resonance characteristic of a hydrogen on the higher-coordinate C4 cage carbon and the lower-field (6.63 ppm) resonance in the range expected for a hydrogen on the lower-coordinate C3 cage carbon.[1]

The structural determination of **3** shown in Figure 1 confirmed the formation of a hybrid *ansa*-cyclopentadienyl-ferratricarbadecaboranyl sandwich complex, where the ring and cage are linked by the *ansa*-CH_2CH_2- group with attachment to the cage at the C2 carbon. Consistent with its 24 skeletal electron count, the ferratricarbadecaborane cluster fragment adopts a *closo*-octadecahedral structure with the iron occupying the unique six-coordinate position above the puckered C2−B5−B6−C3−B7−C4 face. The structure is quite similar to that previously determined for (1-η^5-C_5H_5)-*closo*-2-CH_3-1,2,3,4-$C_3B_7H_9$)Fe with the Cp-ring and the (C4−B5−B6−B7) planes being reasonably parallel in both complexes.[1a] However, in (1-η^5-C_5H_5)-*closo*-2-CH_3-1,2,3,4-$C_3B_7H_9$)Fe the Cp-ring is slightly tilted toward C3, whereas in **3** it is tilted 7(1)° toward the C2 carbon. Likewise, in (1-η^5-C_5H_5)-*closo*-2-CH_3-1,2,3,4-$C_3B_7H_9$) Fe the Fe−C2 (1.968(2) Å) distance is longer than the Fe−C3 (1.947(2) Å) distance, whereas in **3** the Fe−C2 distances is shorter (1.9442(15) Å) than that of Fe−C3 (1.9546(14) Å). Both the Fe1−$Cp_{centroid}$ (1.6758(2) Å) and Fe1−(C4−B5−B6−

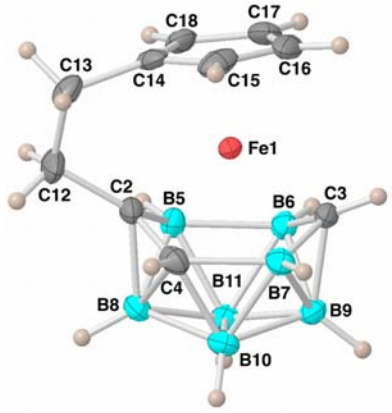

Figure 1. Crystallographically determined structure of **3**. Selected distances (Å) and angles (°): Fe1−C2, 1.9442(15); Fe1−C3, 1.9546(14); Fe1−C4, 2.2325(15); Fe1−B5, 2.2285(17); Fe1−B6, 2.2267(16); Fe1−B7, 2.2652(17); Fe1−$Cp_{centroid}$, 1.6758(2); Fe1−(C4−B5−B6−B7)$_{centroid}$, 1.5964(2); C2−B5, 1.581(2); B5−B6, 1.843(2); C3−B6, 1.583(2); C3−B7, 1.574(2); C4−B7, 1.759(2); C2−C4, 1.498(2); C2−C12, 1.522(2); C12−C13, 1.492(3); C13−C14, 1.529(3); C3−Fe1−C2, 112.24(6); Fe1−C2−C12, 116.68(11); C2−C12−C13, 111.13(16); C12−C13−C14, 108.9(3).

B7)$_{centriod}$ (1.5964(2) Å) distances in **3** are also shorter than those found for (1-η^5-C_5H_5)-*closo*-2-CH_3-1,2,3,4-$C_3B_7H_9$)Fe, Fe−$Cp_{centroid}$ (1.6866(2) Å) and Fe−(C4−B5−B6−B7)$_{centroid}$ (1.6172(2) Å). All of these structural differences are consistent with the *ansa*-ligated unit increasing the iron-bonding interactions with the C2 carbon as well as both of the ring and cluster fragments.

Consistent with the presence of the different isomeric forms of the linked bis-cage dianion shown in Scheme 2, the reaction of **2** with $FeCl_2$ produced the mixture of isomeric *ansa*-$(CH_2)_2$-bistricarbadecaboranyl iron complexes shown in Scheme 3 (bottom). The complexes were easily separated by either chromatography or selective crystallization.

Complex **4** showed only seven equal-intensity resonances in its ^{11}B NMR spectrum (Figure 2, top) and only two cage CH resonances in its ^{1}H NMR spectrum, with both spectra thus

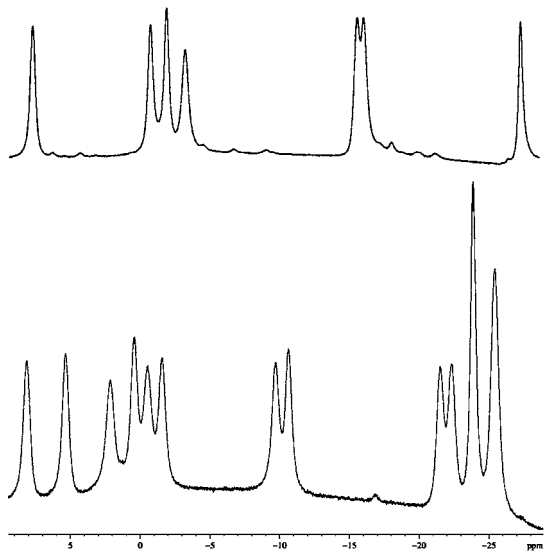

Figure 2. ^{11}B{^{1}H} NMR spectra of **4** (top) and **5** (bottom).

dx.doi.org/10.1021/ja405977q | J. Am. Chem. Soc. 2013, 135, 12407−12413

indicating that the two cages in **4** were symmetry related. These spectra are similar to those previously reported for the *commo*-Fe-(1-Fe-2-CH_3-2,3,5-$C_3B_7H_9$)$_2$ complex that was shown to have two symmetry equivalent cages.[1b]

As shown by the crystallographic determination presented in Figure 3, the iron in **4** is sandwiched between two

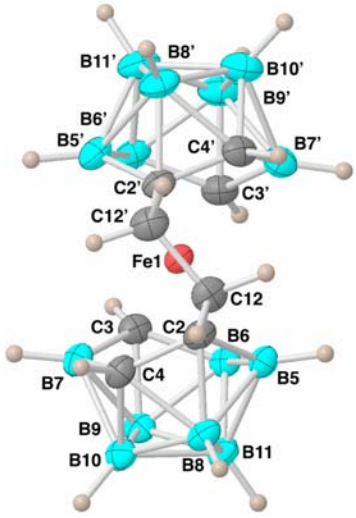

Figure 3. Crystallographically determined structure of **4**. Selected distances (Å) and angles (°): Fe1−C2, 2.0468(13); Fe1−C3, 1.9428(13); Fe1−C4, 2.24961(14); Fe1−B5, 2.2684(16); Fe1−B6, 2.2534(15); Fe1−B7, 2.3828(17); Fe1−(C4−B5−B6−B7)$_{centroid}$, 1.7354(2); Fe1−(C4′−B5′−B6′−B7′)$_{centroid}$, 1.7169(2); C2−B5, 1.591(2); B5−B6, 1.842(2); C3−B6, 1.601(2); C3−B7, 1.578(2); C4−B7, 1.712(2); C2−C4, 1.482(2); C2−C12, 1.5153(18); C12−C12′, 1.540(2); C12′−C2′, 1.5168(19); Fe1−C2′, 2.0288(13); Fe1−C3′, 1.9439(14); Fe1−C4′, 2.4180(14); Fe1−B5′, 2.2926(16); Fe1−B6′, 2.2682(16); Fe1−B7′, 2.3502(17); C2′−B5′, 1.584(2); B5′−B6′, 1.856(2); C3′−B6′, 1.589(2); C3′−B7′, 1.573(2); C4′−B7′, 1.722(2); C2′−C4′, 1.480(2); C3−Fe1−C2, 103.83(6); C3′−Fe1−C2′, 105.21(6); Fe1−C2−C12, 115.69(10); C2−C12−C12′, 105.30(12); C12−C12′−C2′, 105.36(11); C2′−Fe1−C4, 89.09(5); C3′−Fe1−B6, 85.59(6).

tricarbadecaboranyl ligands that are linked by the -CH_2CH_2- group attached at their C2 and C2′ carbons. As can be seen in Figure 3, there is a noncrystallographic C_2 rotation-axis bisecting the -CH_2CH_2- group that equates the two cages. The structure observed for **4**, with the C4 and C4′ carbons on the opposite sides of the two cages, is that which would be expected to result from the reaction of the $FeCl_2$ with one of the RR or SS isomers of **2** shown in Scheme 2.

The iron in **4** occupies the six-coordinate position in each cage with the C4−B5−B6−B7 and C4′−B5′−B6′−B7′ planes in the two cages being nearly parallel, but again slightly tilted toward the tether side by 6.4(3)°. A structural determination[1b] of the related, but nonlinked, *commo*-Fe-(1-Fe-2-CH_3-2,3,5-$C_3B_7H_9$)$_2$ complex showed that the two cages have a nearly staggered conformation with a dihedral angle between the C2−Fe−C3 and C2′−Fe−C3′ planes of 75.1°; however, in **4** the *ansa*-tether constrains cage rotation, and the two cages are forced to adopt a more eclipsed formation with only a 38.92(7)° angle between the C2−Fe−C3 and C2′−Fe−C3′ planes. This constraint results in relatively short C2−C2′ (2.591(2) Å) and C3−C3′ (2.707(2) Å) intercage distances, and these unfavorable interactions between the two cages in **4** are undoubtedly the cause of the observed increases in its Fe1−(C4−B5−B6−B7)$_{centroid}$ (1.7354(2) Å) and Fe1−(C4′−B5′−B6′−B7′)$_{centroid}$ (1.7169(2) Å) distances as well as the considerable lengthening of its Fe1−C2 distance (2.0468(13) Å) compared to those distances found in **3** and *commo*-Fe-(1-Fe-2-CH_3-2,3,5-$C_3B_7H_9$)$_2$ (Fe-*centroid*: 1.70614(4) Å).

Both **5** and **6** showed more complex ^{11}B and ^{1}H NMR spectra than **4**, indicating that the two linked cages in these complexes were not equivalent. Thus, the ^{11}B NMR spectra of **5** (Figure 2, bottom) and **6** exhibited 1:1:1:1:1:1:1:1:1:1:2:2 and 1:1:2:1:1:1:1:1:2:1:1:1 patterns, respectively, and their ^{1}H NMR spectra each exhibited four separate cage-CH resonances. Most significantly, for both compounds, three of the cage-CH resonances appeared at the lower-field shifts characteristic of a C2H or C3H cage hydrogen, and only one resonance was found in the higher-field region expected for a C4H cage hydrogen. These differences suggest that the two cages in **5** and **6** were linked differently than **4**. This conclusion was confirmed by the crystallographic determinations depicted in Figures 4 and 5.

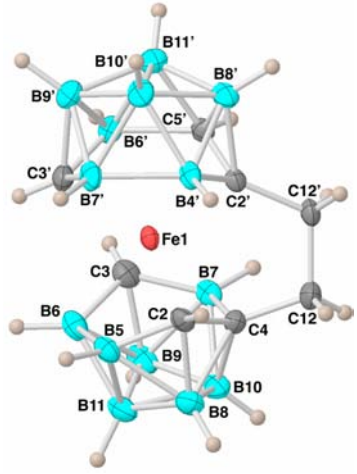

Figure 4. Crystallographically determined structure of **5**. Selected distances (Å) and angles (°): Fe1−C2, 1.9598(19); Fe1−C3, 1.9807(19); Fe1−C4, 2.2169(19); Fe1−B5, 2.317(2); Fe1−B6, 2.369(2); Fe1−B7, 2.235(2); Fe1−(C4−B5−B6−B7)$_{centroid}$, 1.6543(2); Fe1−(B4′−C5′−B6′−B7′)$_{centroid}$, 1.6680(2); C2−B5, 1.561(3); B5−B6, 1.853(3); C3−B6, 1.566(3); C3−B7, 1.572(3); C4−B7, 1.764(3); C2−C4, 1.494(2); C4−C12, 1.522(3); C12−C12′, 1.532(3); C12′−C2′, 1.529(2); Fe1−C2′, 1.9882(17); Fe1−C3′, 1.9555(19); Fe1−C5′, 2.2771(19); Fe1−B4′, 2.332(2); Fe1−B7′, 2.274(2); Fe1−B6′, 2.291(2); C2−B4′, 1.584(3); B4′−B7′, 1.861(3); C3′−B7′, 1.581(3); C3′−B6′, 1.581(3); C5′−B6′, 1.751(3); C2′−C5′, 1.501(3); C3−Fe1−C2, 108.36(9); C3′−Fe1−C2′, 109.28(8); Fe1−C4−C12, 115.07(13); C4−C12−C12′, 108.61(16); C12−C12′−C2′, 113.14; C2′−Fe1−C4, 79.21(7); C3′−Fe1−B6 86.73(9).

In both **5** and **6**, the two cages are no longer linked at the C2 and C2′ positions found in **4** but rather at the C2 and C4′ cage-carbons. The **5** and **6** structures differ only in handedness of the cages. Thus, as can be seen by comparing Figures 4 and 5, in compound **5**, the C4 and C5′ carbons are on opposite sides of the tether, whereas in compound **6** the C4 and C4′ carbons are on the same side. The change of one cage-linkage position to the C4-carbon allows the two cages in both **5** and **6** to adopt more staggered conformations than was found for **4**, with the dihedral angles between the C2−Fe1−C3 and C2′−Fe1−C3′ planes in the two compounds being increased to 64.04(5)° and

dx.doi.org/10.1021/ja405977q | J. Am. Chem. Soc. 2013, 135, 12407−12413

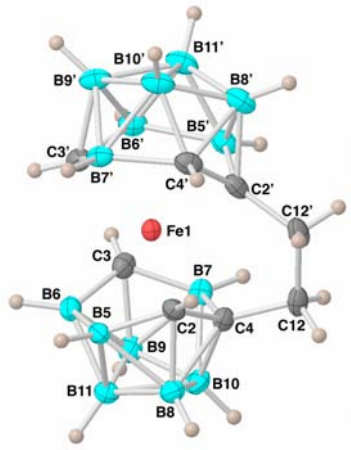

Figure 5. Crystallographically determined structure of **6**. Selected distances (Å) and angles (°): Fe1−C2, 1.9736(14); Fe1−C3, 1.9662(14); Fe1−C4, 2.2247(13); Fe1−B5, 2.3771(15); Fe1−B6, 2.3632(16); Fe1−B7, 2.2329(16); Fe1−$(C4-B5-B6-B7)_{centroid}$, 1.6702(1); Fe1−$(C4'-B5'-B6'-B7')_{centroid}$, 1.6937(1); C2−B5, 1.559(2); B5−B6, 1.841(2); C3−B6, 1.579(2); C3−B7, 1.580(2); C4−B7, 1.772(2); C2−C4, 1.4953(19); C4−C12, 1.5134(19); C12−C12′, 1.534(2); C12′−C2′, 1.530(2); Fe1−C2′, 2.0044(13); Fe1−C3′, 1.9584(14); Fe1−C4′, 2.3618(14); Fe1−B5′, 2.2795(16); Fe1−B6′, 2.3040(16); Fe1−B7′, 2.3021(15); C2′−B5′, 1.583(2); B5′−B6′, 1.852(2); C3′−B6′, 1.588(2); C3′−B7′, 1.575(2); C4′−B7′, 1.748(2); C2′−C4′, 1.495(2); C3−Fe1−C2, 107.08(6); C3′−Fe1−C2′, 107.53(6); Fe1−C4−C12, 114.69(13); C4−C12−C12′, 108.17(12); C12−C12′−C2′, 113.23(12); C2′−Fe1−C4, 78.96(6); C3′−Fe1−B6, 88.30(6).

56.36(4)°, respectively. These more staggered configurations result in a decrease in the unfavorable intercage interactions, as can be seen in the increases in the C2−C2′ (**5**, 2.817(2); **6** 2.711(2) Å) and C3−C3′ (**5**, 2.890(2); **6**, 2.839(2) Å) distances relative to those of **4**. The attachment of the tether at the C4-carbon also enhances the iron cluster bonding since the iron in these complexes can more closely approach their C4−B5−B6−B7 bonding faces (**5**, Fe1−$(C4-B5-B6-B7)_{centroid}$, 1.6543(2) Å and Fe1−$(B4'-C5'-B6'-B7')_{centroid}$, 1.6680(2) Å; **6**, Fe1−$(C4-B5-B6-B7)_{centroid}$, 1.6702(1) Å and Fe1−$(C4'-B5'-B6'-B7')_{centroid}$, 1.6937(1) Å) than was possible in **4**.

The formation of the structures observed for **5** and **6** is consistent with our previous observation that the (1-η^5-C_5H_5)-*closo*-2-CH_3-1,2,3,4-$C_3B_7H_9$)Fe complex will readily isomerize under mild conditions to its (1-η^5-C_5H_5)-*closo*-4-CH_3-1,2,3,4-$C_3B_7H_9$)Fe isomer.[1b,c] In this earlier work, we also used ^{13}C labeling studies to show[1c] that the isomerization could occur by a simple C2−C5−B10−B11−B13 belt rotation mechanism, with the C2 carbon moving to the C4 position while retaining its exopolyhedral methyl-substituent. Such a process can also readily account for the formation of **5** and **6**. As shown in Scheme 4 (top), the structure observed for **5** can be derived in a straightforward manner from **4** by a simple rotation of the C4−C2−B5−B11−B10 belt in **4**, with C4 moving to C2 and the tether-attached C2 moving to the 5-positon with its tether bond staying intact. The conversion of **4** to **5** was experimentally confirmed in a separate experiment, where heating a sample of **4** at 200 °C for 8 h resulted in a complete conversion to **5**.

As shown in Scheme 4 (bottom), a simple belt rotation mechanism starting with isomer **4′** could also account for the

Scheme 4. Conversion of 4 to 5 and 4′ to 6 by Belt Rotation Mechanisms

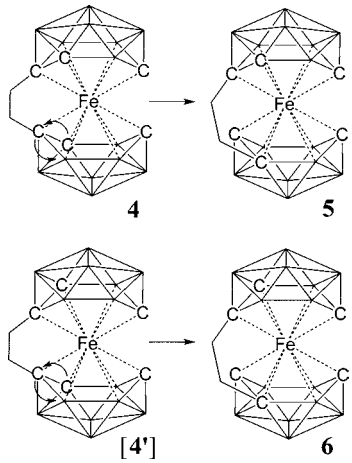

formation of **6**. However, although isomer **4′** should have been produced by the reaction of $FeCl_2$ with the RS isomer of **2** that is shown in Scheme 2, it was never observed as a reaction product. Its absence as a product in these reactions suggests that the steric interactions in such a structure, similar to those observed for **4**, must be significant and result in **4′** readily isomerizing to **6**.

In summary, in this paper we have reported the syntheses and structural characterizations of the first examples of a new class of inorganic *ansa*-metallocene-like clusters: the *ansa*-metallatricarbadecaboranes. Furthermore, the structural studies of these complexes have clearly demonstrated that, depending upon the linking-position of the *ansa*-tether, constraints in cage orientation, such as observed in **4**, produce unfavorable intercage steric interactions. However, the cage fragments in these complexes can readily undergo a cage carbon migration that moves one C2-carbon and its tether linkage to the more favorable 4-position. This isomerization reduces the cage steric interactions and produces configurations, such as those found for **5** and **6**, where the iron cage bonding is enhanced as a result of the binding effect of the tether. These studies also suggest that the properties of these complexes can be further tuned by adjusting the length of the *ansa*-linkage to allow more flexible cage orientations while still retaining the beneficial bonding enhancement of the *ansa*-linkage. We are presently exploring these possibilities.

■ ASSOCIATED CONTENT

Supporting Information

X-ray crystallographic data for the structural determinations of **3**−**6** (CIF). These materials are available free of charge via the Internet at http://pubs.acs.org.

■ AUTHOR INFORMATION

Corresponding Author

lsneddon@sas.upenn.edu

Notes

The authors declare no competing financial interest.

■ ACKNOWLEDGMENTS

The National Science Foundation is gratefully acknowledged both for the support of this research and for an instrumentation

grant (CHE-0840438) that was used for the purchase of the X-ray diffractometer employed in these studies.

REFERENCES

(1) (a) Plumb, C. A.; Carroll, P. J.; Sneddon, L. G. *Organometallics* **1992**, *11*, 1665−1671. (b) Plumb, C. A.; Carroll, P. J.; Sneddon, L. G. *Organometallics* **1992**, *11*, 1672−1680. (c) Plumb, C. A.; Carroll, P. J.; Sneddon, L. G. *Organometallics* **1992**, *11*, 1681−1685. (d) Weinmann, W.; Wolf, A.; Pritzkow, H.; Siebert, W.; Barnum, B. A.; Carroll, P. J.; Sneddon, L. G. *Organometallics* **1995**, *14*, 1911−1919. (e) Barnum, B. A.; Carroll, P. J.; Sneddon, L. G. *Organometallics* **1996**, *15*, 645−654. (f) Barnum, B. A.; Carroll, P. J.; Sneddon, L. G. *Inorg. Chem.* **1997**, *36*, 1327−1337. (g) Wasczak, M. D.; Lee, C. C.; Hall, I. H.; Carroll, P. J.; Sneddon, L. G. *Angew. Chem., Int. Ed. Engl.* **1997**, *36*, 2228−2230. (h) Ramachandran, B. M.; Carroll, P. J.; Sneddon, L. G. *J. Am. Chem. Soc.* **2000**, *122*, 11033−11034. (i) Wasczak, M. D.; Wang, Y.; Garg, A.; Geiger, W. E.; Kang, S. O.; Carroll, P. J.; Sneddon, L. G. *J. Am. Chem. Soc.* **2001**, *123*, 2783−2790. (j) Ramachandran, B. M.; Trupia, S. M.; Geiger, W. E.; Carroll, P. J.; Sneddon, L. G. *Organometallics* **2002**, *21*, 5078−5090. (k) Hall, I. H.; Durham, R.; Tran, M.; Mueller, S.; Ramachandran, B. M.; Sneddon, L. G. *J. Inorg. Biochem.* **2003**, *93*, 125−131. (l) Ramachandran, B. M.; Carroll, P. J.; Sneddon, L. G. *Inorg. Chem.* **2004**, *43*, 3467−3474. (m) Ramachandran, B. M.; Wang, Y.; Kang, S. O.; Carroll, P. J.; Sneddon, L. G. *Organometallics* **2004**, *23*, 2989−2994. (n) Butterick, R., III; Ramachandran, B. M.; Carroll, P. J.; Sneddon, L. G. *J. Am. Chem. Soc.* **2006**, *128*, 8626−8637. (o) Nafady, A.; Butterick, R., III; Calhorda, M. J.; Carroll, P. J.; Chong, D.; Geiger, W. E.; Sneddon, L. G. *Organometallics* **2007**, *26*, 4471−4482. (p) Butterick, R., III; Carroll, P. J.; Sneddon, L. G. *Organometallics* **2008**, *27*, 4419−4427. (q) Stewart, M.; Butterick, R., III; Sneddon, L. G.; Matsuo, Y.; Geiger, W. E. *Inorg. Chim. Acta* **2010**, *364*, 251−254. (r) Perez-Gavilan, A.; Carroll, P. J.; Sneddon, L. G. *Collect. Czech. Chem. Commun.* **2010**, *75*, 905−917. (s) Perez-Gavilan, A.; Carroll, P. J.; Sneddon, L. G. *Organometallics* **2012**, *31*, 2741−2748. (t) Perez-Gavilan, A.; Carroll, P. J.; Sneddon, L. G. *Inorg. Chem.* **2012**, *51*, 5903−5910. (u) Perez-Gavilan, A.; Carroll, P. J.; Sneddon, L. G. *J. Organomet. Chem.* **2012**, *721*−*722*, 62−69. (v) Gleeson, B.; Carroll, P. J.; Sneddon, L. G. *J. Organomet. Chem.* **2012**, http://dx.doi.org/10.1016/j.jorganchem.2012.12.001.

(2) For some general references on the properties of *ansa*-Cp complexes, see: (a) Shapiro, P. J. *Coord. Chem. Rev.* **2002**, *231*, 67−81. (b) Prashara, S.; Nolo, A. A.; Otero, A. *Coord. Chem. Rev.* **2006**, *250*, 133−154. (c) Wang, B. *Coord. Chem. Rev.* **2006**, *250*, 242−258. (d) Erker, G. *Macromol. Symp.* **2006**, *236*, 1−13.

(3) For some examples of *ansa*-metalladicarbaboranyl complexes see: (a) Wang, Y.; Wang, H.; Li, H.-W.; Xie, Z. *Organometallics* **2002**, *21*, 3311−3313. (b) Xie, Z. *Acc. Chem. Res.* **2003**, *36*, 1−9. (c) Wang, Y.; Liu, D.; Chan, H.-S.; Xie, Z. *Organometallics* **2008**, *27*, 2825−2832. (d) Liu, D.; Wang, Y.; Chan, H.-S.; Tang, Y.; Xie, Z. *Organometallics* **2008**, *27*, 5295−5302. (e) Sit, M.-M.; Chan, H.-S.; Xie, Z. *Organometallics* **2009**, *28*, 5998−6002.

(4) Shriver, D. F.; Drezdzon, M. A. *Manipulation of Air-Sensitive Compounds*; 2nd ed.; Wiley: New York, 1986.

(5) Leong, W. L. J.; Garland, M. V.; Goh, L. Y.; Leong, W. K. *Inorg. Chim. Acta* **2009**, *362*, 2089−2092.

(6) (a) Hawthorne, M. F.; Young, D. C.; Garrett, P. M.; Owen, D. A.; Schwerin, S. G.; Tebbe, F. N.; Wegner, P. A. *J. Am. Chem. Soc.* **1968**, *90*, 862−868. (b) Garrett, P. M.; George, T. A.; Hawthorne, M. F. *Inorg. Chem.* **1969**, *8*, 2008−2009.

(7) *SAINT*, version 7.68A; Bruker AXS, Inc.: Madison, WI, 2009.

(8) *SHELXTL*, version 6.14; Bruker AXS, Inc.: Madison, WI, 2003.

(9) SIR97: Altomare, A.; Burla, M. C.; Camalli, M.; Cascarano, M.; Giacovazzo, C.; Guagliardi, A.; Moliterni, A.; Polidori, G. J.; Spagna, R. *J. Appl. Crystallogr.* **1999**, *32*, 115−119.

(10) Sheldrick, G. M. *Acta Crystallogr.* **2008**, *A64*, 112−122.

(11) Kang, S. O.; Furst, G. T.; Sneddon, L. G. *Inorg. Chem.* **1989**, *28*, 2339−2347.